

# Isotropic-nematic transition in liquid crystals confined between rough walls

D. L. Cheung<sup>1</sup> and F. Schmid<sup>2</sup>

<sup>1</sup>*Department of Physics and Centre for Scientific Computing,  
University of Warwick, Coventry, CV4 7AL, UK\**

<sup>2</sup>*Fakultät für Physik, Universität, Bielefeld, 33615 Bielefeld, Germany*

The effect of rough walls on the phase behaviour of a confined liquid crystal (LC) fluid is studied using constant pressure Monte Carlo simulations. The LC is modelled as a fluid of soft ellipsoidal molecules and the rough walls are represented as a hard wall with a number of molecules randomly embedded in them. It is found that the isotropic-nematic (IN) transition is shifted to higher pressures for rougher walls.

## I. INTRODUCTION

The phase behaviour of many fluids alters when they are confined<sup>1</sup>. This is particularly true for ordered fluids such as liquid crystals (LC)<sup>2</sup>. As well as being interesting in its own right, the effect of confinement LCs is of technological significance. Many applications of LCs depend crucially on this interaction.

Because of this interest there have been many studies of confined LCs. Simulations have studied many aspects of the effect of confinement on LCs, such as wetting behaviour<sup>3</sup> and anchoring strength<sup>4</sup>. The effect of confinement on the phase behaviour has also been studied<sup>5,6</sup>. In a recent paper the effect of rough walls on the behaviour of confined LCs was examined<sup>7</sup>. Specifically the structure of the fluid and the surface anchoring was studied. It was found that the surface anchoring became weaker as the surfaces became rougher, which may have implications for the phase behaviour of the confined fluid. The aim of the present paper is to study the effect of rough surfaces on the isotropic-nematic (IN) transition of a confined LC.

## II. MODEL AND SIMULATION DETAILS

In order to simulate both a large number of fluid molecules for a reasonable range of pressures and wall roughnesses simple models for both the molecule-molecule and molecule-wall interactions are used.

A simplified version of the Gay-Berne (GB) potential<sup>8</sup> is employed. The interaction between two molecules  $i$  and  $j$ , with positions  $\mathbf{r}_i$  and  $\mathbf{r}_j$ , and orientations  $\mathbf{u}_i$  and  $\mathbf{u}_j$  is given by

$$V(\mathbf{r}_{ij}, \mathbf{u}_i, \mathbf{u}_j) = \begin{cases} 4\epsilon_0 [\rho^{-12} - \rho^{-6}] + \epsilon_0, & \rho \leq 2^{1/6} \\ 0, & \text{otherwise} \end{cases} \quad (1)$$

where  $\mathbf{r}_{ij} = \mathbf{r}_i - \mathbf{r}_j$  and

$$\rho(\mathbf{r}_{ij}, \mathbf{u}_i, \mathbf{u}_j) = \frac{r_{ij} - \sigma(\hat{\mathbf{r}}_{ij}, \mathbf{u}_i, \mathbf{u}_j) + \sigma_0}{\sigma_0}. \quad (2)$$

$r_{ij} = |\mathbf{r}_{ij}|$ , and  $\hat{\mathbf{r}}_{ij} = \mathbf{r}_{ij}/r_{ij}$ .  $\sigma_0$  is the molecular width, which defines the length scale used throughout this pa-

per.  $\sigma(\hat{\mathbf{r}}_{ij}, \mathbf{u}_i, \mathbf{u}_j)$  is the shape function given by<sup>9</sup>

$$\sigma(\hat{\mathbf{r}}_{ij}, \mathbf{u}_i, \mathbf{u}_j) = \sigma_0 \left\{ 1 - \frac{\chi}{2} \left[ \frac{(\hat{\mathbf{r}}_{ij} \cdot \mathbf{u}_i + \hat{\mathbf{r}}_{ij} \cdot \mathbf{u}_j)^2}{1 + \chi \mathbf{u}_i \cdot \mathbf{u}_j} + \frac{(\hat{\mathbf{r}}_{ij} \cdot \mathbf{u}_i - \hat{\mathbf{r}}_{ij} \cdot \mathbf{u}_j)^2}{1 - \chi \mathbf{u}_i \cdot \mathbf{u}_j} \right] \right\}^{-1/2} \quad (3)$$

where  $\chi = (\kappa^2 - 1)/(\kappa^2 + 1)$ , with the elongation  $\kappa = 3$ . This approximates the contact distance between two ellipsoids.  $\epsilon_0$  and  $\sigma_0$  define the energy and length scales used throughout this paper, with other quantities given in terms of these. Specifically the reduced pressure is  $P^* = P\sigma_0^3/\epsilon_0$  and the reduced temperature is  $T^* = k_B T/\epsilon_0$ . As the potential is fully repulsive, temperature is not a significant variable and is set  $T^* = 0.5$  throughout.

The walls are represented by a hard core potential acting on the centres of mass of the fluid molecules, giving rise to homeotropic anchoring. Roughness is introduced by embedding some molecules in the wall<sup>7</sup>. These are given random positions in the  $xy$  plane and random orientations which are held fixed during the simulations. It should be noted that these are used as a convenient method to introduce disorder into the surface-molecule interaction and do not correspond to real molecules. The roughness of the wall is characterised by the density of these embedded molecules  $\Sigma$ .

As the aim of this study is to investigate the phase behaviour, constant  $NPT$  simulations are more appropriate than constant  $NVT$  simulations<sup>10</sup>. To retain a constant  $\Sigma$ , volume moves involve only changes in the  $z$  box length. The phase behaviour is probed using a series of simulations at different pressures, starting from a high pressure  $P^* = 2.50$  in the nematic phase. The simulated systems comprised 1200 fluid molecules and up to 60 molecules in the walls. The fixed area of each wall was  $154.9 \sigma_0^2$ . The cell width was in the range 22 - 28  $\sigma_0$ . To ensure some sampling of surface configurations three different walls were studied for each value of  $\Sigma$ . The order parameters and directors for these are presented in Tab. 1.

Table 1.

Order parameter and directors for the wall configurations studied.

$\Sigma$	$S_2^{wall}$	$\mathbf{n}^{wall}$
0.1	1 0.165	( 0.261,-0.560, 0.786)
	2 0.181	(-0.520, 0.404,-0.753)
	3 0.145	(-0.392,-0.919, 0.035)
0.2	1 0.153	( 0.013, 0.054, 0.952)
	2 0.304	( 0.638, 0.661, 0.396)
	3 0.235	(-0.338,-0.937, 0.089)
0.3	1 0.217	( 0.051,-0.177, 0.983)
	2 0.220	( 0.963, 0.016, 0.268)
	3 0.160	( 0.009, 0.992, 0.128)
0.4	1 0.329	(-0.745, 0.035, 0.666)
	2 0.382	(-0.884, 0.539, 0.121)
	3 0.262	(-0.062,-0.329, 0.942)

Due to the number of different systems considered (3 for each non-zero  $\Sigma$  and one smooth wall) only a coarse sampling of pressure is attempted; the pressure being changed in steps of 0.02 (in reduced units) near the NI transition. This limits the accuracy at which transition pressures may be determined. While techniques such as Gibbs Ensemble Monte Carlo (GEMC)<sup>11,12</sup> or grand canonical Monte Carlo (GCMC)<sup>10</sup> simulations may be used to investigate phase equilibria the densities involved lead to unacceptably low acceptance rates for particle transfers. Studying more elongated molecules<sup>13,14</sup> (with lower  $\rho_{NI}$ ) or softer interaction models<sup>15</sup> would allow the use of these techniques.

As the nematic phase has orientational order which is lacking in the isotropic phase, the phase of the system may be determined by calculating the orientational order parameter. This is given by the largest eigenvalue of the ordering tensor

$$Q_{\alpha\beta} = \sum_{i=1}^N \left( \frac{3}{2} u_{i\alpha} u_{i\beta} - \frac{1}{2} \delta_{\alpha\beta} \right) \quad (4)$$

where  $\delta_{\alpha\beta}$  is the Kronecker delta function. The order parameter  $S_2$  is then determined by diagonalising this. For a nematic  $S_2$  is typically  $> 0.4$ , while lower values are typical of an isotropic state.

As the presence of surfaces gives rise to an inhomogeneous distribution of molecules it is useful to consider quantities such as the density or order parameter in different regions of the simulation cell. As previous studies indicate that a layer of well ordered molecules forms even for rough walls<sup>7</sup>, the order parameter in the central half of the cell  $S_2^{bulk}$  ( $l_z/4$  to  $3l_z/4$ ) may be taken to be the most useful variable for characterising the phase of the confined fluid. The variation of density and order may be examined more closely by the density and order parameter profiles.

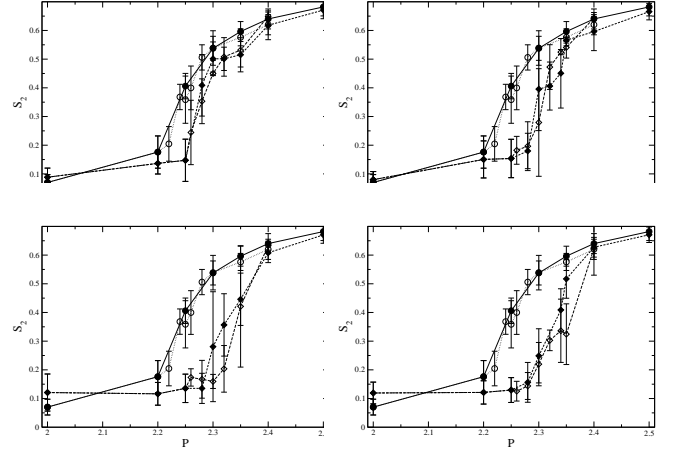


FIG. 1: Variation of bulk order parameter with pressure. Solid line with filled circles shows  $\Sigma = 0.0$  (expansion), dotted line with open circles shows  $\Sigma = 0.0$ , dashed line with filled diamonds shows (a)  $\Sigma = 0.1$ , (b)  $\Sigma = 0.2$ , (c)  $\Sigma = 0.3$ , and (d)  $\Sigma = 0.4$  (expansion) and the long dashed line with open diamonds shows (a)  $\Sigma = 0.1$ , (b)  $\Sigma = 0.2$ , (c)  $\Sigma = 0.3$ , and (d)  $\Sigma = 0.4$  (compression).

### III. RESULTS AND DISCUSSION

#### A. Phase behaviour

Shown in Fig. 1  $S_2^{bulk}$  as a function of  $P$ . As can be seen, on expansion  $S_2^{bulk}$  gradually decreases until  $P^* = 2.25$  ( $S_2^{bulk} \approx 0.4$ ), before falling to an isotropic state at  $P^* = 2.20$ . For this system the bulk isotropic-nematic transition occurs at  $P_{NI}^{*bulk} = 2.30$ <sup>16</sup>. Note that due to finite size effects the order parameter does not go exactly to 0<sup>17</sup>. The system shows a similar transition on compression for an isotropic starting state. The lowering of  $P_{NI}$  relative to the bulk phase is caused by the formation of a highly ordered layer near the walls<sup>6,18</sup>.

This behaviour is similar to the rough wall with  $\Sigma = 0.1$  (Fig. 1a). However, the NI transition seems to be shifted to a higher pressure (between  $P^* = 2.25$  and  $P^* = 2.30$ ). Away from the transition the behaviour of  $S_2^{bulk}$  is similar to that of the smooth wall system. For pressures above the  $P_{BulkNI}$  the fluid in the cell bulk would be nematic anyway so the rough walls would have little effect on  $S_2^{bulk}$  in this case, while for  $P$  much less than  $P_{NI}$  the anchoring effect of the walls is insufficient to lead to ordering in the cell bulk.

The effect of further increasing the surface roughness may be seen in Fig. 1b, which shows  $S_2^{bulk}$  against  $P^*$  for the  $\Sigma = 0.2$  wall. As may be seen the NI transition is shifted to a high pressure compared to the  $\Sigma = 0.1$  wall ( $P_{NI}^* \approx 2.30$ ). Figure 1(c) and (d) show the phase diagram for walls with  $\Sigma = 0.3$  and  $\Sigma = 0.4$  respectively. While  $P_{NI}$  increases on going from  $\Sigma = 0.2$  to  $\Sigma = 0.3$ , there is a much smaller difference between  $\Sigma = 0.3$  and  $\Sigma = 0.4$ , suggesting that the effect of the rough walls becomes saturated with increasing roughness, similar to

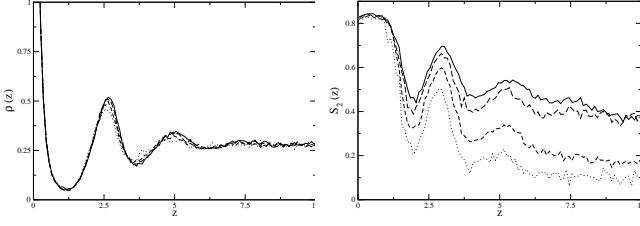


FIG. 2: (a) Density profiles for the smooth wall system. Solid line is  $P^* = 2.25$  (expansion), dotted line is  $P^* = 2.20$  (expansion), dashed line is  $P^* = 2.22$  (compression), and dot-dashed line is  $P^* = 2.26$  (compression) (b) Order parameter profiles for smooth wall system. Symbols as in (a).

the anchoring coefficient<sup>7</sup>. The change in order parameter through the NI transition also appears to become smoother as  $\Sigma$  increases. This may be due to averaging over different wall configurations as these may have different  $P_{NI}$ . This change in the location of the IN transition may also be seen from the large error bars for  $S_2^{bulk}$  for pressures near  $P_{NI}$ .

The approximate transition pressures and order parameters are presented in Tab. 2. These generally increase with surface roughness. This may be attributed to the rough walls disturbing the highly ordered surface layer, which disrupts the order in the bulk. This can also be seen from the decrease in the surface anchoring strength as  $\Sigma$  increases<sup>7</sup>.

Table 2.

Approximate transition pressures and order parameters. Errors in the final decimal place are in parentheses

$\Sigma$	$P_N^{exp}$	$P_I^{exp}$	$P_N^{cmp}$	$P_I^{cmp}$	$S_2^{Nexp}$	$S_2^{Iexp}$	$S_2^{Ncmp}$	$S_2^{Icmp}$
0.0	2.25	2.20	2.26	2.22	0.41(4)	0.18(6)	0.40(7)	0.20(6)
0.1	2.30	2.25	2.30	2.25	0.50(6)	0.15(7)	0.45(1)	0.15(7)
0.2	2.35	2.25	2.34	2.30	0.57(1)	0.15(7)	0.52(9)	0.20(8)
0.3	2.40	2.28	2.40	2.30	0.61(3)	0.14(5)	0.63(2)	0.16(2)
0.4	2.35	2.28	2.40	2.28	0.52(7)	0.16(7)	0.62(9)	0.14(5)

## B. Fluid Structure

Shown in Fig. 2a are density profiles for the smooth wall system. These are shown for pressures just above and below the isotropic-nematic transition for both expansion and compression (for the expansion runs these are  $P_{nem} = 2.25$  and  $P_{iso} = 2.20$  and for the compression runs  $P_{nem} = 2.26$  and  $P_{iso} = 2.22$ ). As can be seen there is a noticeable decrease in the height of the density peak at around  $z \approx 2.5$  when going from the nematic to isotropic phases ( $P^* = 2.25 \rightarrow 2.20$ ). However, on going from the isotropic to nematic phase ( $P^* = 2.22 \rightarrow 2.26$ ) there is a much smaller change in the density profile.

The order parameter profiles for these pressures are shown in Fig. 2b. For all pressures there is a well ordered layer near the wall, which has similar values for

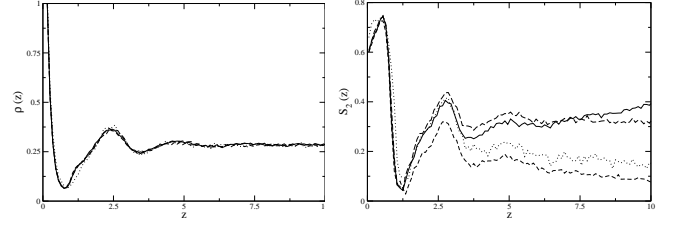


FIG. 3: (a) Density profiles for rough wall with  $\Sigma = 0.2$ . Solid line is  $P^* = 2.30$  (expansion), dotted line is  $P^* = 2.28$  (expansion), dashed line is  $P^* = 2.28$  (compression), and dot-dashed line is  $P^* = 2.32$  (compression) (b) Order parameter profiles for rough wall with  $\Sigma = 0.2$ . Symbols as in (a).

all pressures. More variation is seen around the second peak  $z \approx 2.5$ . For the isotropic fluids the order parameter profile is typically less than 0.1, while for the nematic  $S_2^{bulk}(z) \approx 0.4$ .

Density and order parameter profiles for the rough wall with  $\Sigma = 0.2$  are shown in Fig. 3. The expansion runs are given at  $P_{nem} = 2.30$  and  $P_{iso} = 2.28$  and for the compression runs  $P_{nem} = 2.28$  and  $P_{iso} = 2.32$ . Compared to the smooth wall the density profiles are less structured, with only a single peak at  $z \approx 2.5$  visible for the lowest pressures shown, which also appears wider than the equivalent peak for the smooth wall, due to the disruption of the layer structure due to the surface disorder<sup>19</sup>.

The effect of the rough walls is more prominent for the order parameter profiles (fig. 3b). Near the wall  $S_2^{bulk}(z)$  is significantly lower than for the smooth wall, due to the disordering effect of the wall molecules. The order minima is deeper (the minimum value  $\approx 0.1$  for all pressures shown) and is moved closer to the wall ( $z \approx 1.1$ ). However, this does not extend into the bulk fluid.

Density and order parameter profiles for  $\Sigma = 0.4$  are shown in Fig. 4. Profiles for the expansion runs are at  $P_{nem}^* = 2.35$  and  $P_{iso}^* = 2.28$  and for the compression runs  $P_{nem}^* = 2.28$  and  $P_{iso}^* = 2.40$ . The density profile shows even less structure than for  $\Sigma = 0.2$ , with only a density peak at  $z \approx 2.5$  visible. However, this peak has a broad shoulder starting at  $z \approx 2.0$ , corresponding to molecules lying in the plane of the wall in the region between the two layers<sup>7</sup>. This is similar to the behaviour seen in simulations of smectic LCs<sup>20</sup>. The effect of this bimodal distribution may be seen by the depletion of the order parameter in this region and by a peak in the biaxiality profile (c.f. Fig 2d of Ref.<sup>7</sup>).

## IV. CONCLUSIONS

The phase behaviour of a model liquid crystal confined between two rough walls has been studied. Particular attention is paid to its behaviour in the vicinity of the isotropic-nematic transition.

For smooth walls it is found that the nematic-isotropic transition is shifted to lower pressures compared to the

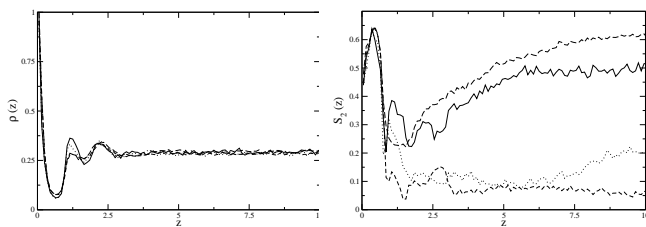


FIG. 4: (a) Density profiles for rough wall with  $\Sigma = 0.4$ . Solid line is  $P^* = 2.35$  (expansion), dotted line is  $P^* = 2.28$  (expansion), dashed line is  $P^* = 2.28$  (compression), and dot-dashed line is  $P^* = 2.40$  (compression) (b) Order parameter profiles for rough wall with  $\Sigma = 0.2$ . Symbols as in (a).

bulk. This may be attributed to the anchoring effect of the walls. As the walls become rougher, this effect is weakened so the transition is shifted to higher pressures. For pressures away from the transition pressure the rough walls appear to have a smaller effect.

On examining the structure of the confined fluid, it is found that the density distribution changes little with pressure, rather changes in this are largely due to increasing wall roughness. The behaviour of the order pa-

rameter near the wall is likewise determined by the wall roughness.

To summarize, we find that surface roughness not only decreases the nematic order in the vicinity of the surface, but also shifts the nematic-isotropic transition to higher pressures in thin slabs. It would be interesting to study other quantities, in particular, the anchoring direction. On flat surfaces, the anchoring direction is homeotropic. On rough surfaces, we observe that the system sometimes switches to planar anchoring. However, this depends sensitively on the particular realization of the disorder, and much more extensive simulations of much larger systems would be necessary to clarify this issue.

### Acknowledgements

Computational resources for this work were provided by the Centre for Scientific Computing of the University of Warwick. The authors wish to acknowledge helpful conversations with Michael Allen and Tanja Schilling. This work was funded by the UK EPSRC.

---

\* Electronic address: david.cheung@warwick.ac.uk

- <sup>1</sup> L. D. Gelb, K. E. Gubbins, R. Radhakrishnan, M. Slwiska-Bartkowiak, Rep. Prog. Phys. 62 (1999) 1573.
- <sup>2</sup> B. Jerome, Rep. Prog. Phys. 54 (1992) 391.
- <sup>3</sup> M. Dijkstra, R. van Roij, R. Evans, Phys. Rev. E 63 (2001) 051703.
- <sup>4</sup> D. Andrienko, M. P. Allen, Phys. Rev. E 65 (2002) 021704.
- <sup>5</sup> J. Quintana, E. C. Poiré, H. Dominguez, J. Alejandro, Mol. Phys. 100 (2002) 2597.
- <sup>6</sup> H. Steuer, S. Hess, M. Schoen, Phys. Rev. E 69 (2004) 031708.
- <sup>7</sup> D. L. Cheung, F. Schmid, J. Chem. Phys. 122 (2005) 074902.
- <sup>8</sup> J. G. Gay, B. J. Berne, J. Chem. Phys. 74 (1981) 3316.
- <sup>9</sup> B. J. Berne, P. Pechukas, J. Chem. Phys. 56 (1975) 4213.
- <sup>10</sup> M. P. Allen, D. J. Tildesley, Computer Simulation of Liq-

uids, OUP, Oxford, 1985.

- <sup>11</sup> A. Z. Panagiotopoulos, Mol. Phys. 61 (1987) 813.
- <sup>12</sup> A. Z. Panagiotopoulos, Mol. Phys. 62 (1987) 709.
- <sup>13</sup> P. J. Camp, C. P. Mason, M. P. Allen, A. A. Khare, D. A. Kofke, J. Chem. Phys. 105 (1995) 2837.
- <sup>14</sup> R. L. C. Vink, S. Wolfsheimer, T. Schilling, J. Chem. Phys. 123 (2005) 074901.
- <sup>15</sup> R. L. C. Vink, T. Schilling, Phys. Rev. E 71 (2005) 051716.
- <sup>16</sup> H. Lange, F. Schmid, Comp. Phys. Comm. 147 (2002) 276.
- <sup>17</sup> R. Eppenga, D. Frenkel, Mol. Phys. 52 (1984) 1303.
- <sup>18</sup> G. D. Wall, D. J. Cleaver, Phys. Rev. E 56 (1997) 4306.
- <sup>19</sup> C. Delattre, W. Dong, J. Chem. Phys. 110 (1999) 570.
- <sup>20</sup> R. von Roij, P. Bolhuis, B. Mulder, D. Frenkel, Phys. Rev. E 52 (1995) 1277.